Available online at www.sciencedirect.com
ScienceDirect
Journal of Molecular Graphics and Modelling 25 (2006) 389–395
Journal of Molecular Graphics and Modelling
www.elsevier.com/locate/JMGM

Computation of through-space NMR shielding effects by small-ring aromatic and antiaromatic hydrocarbons

Ned H. Martin *, David M. Loveless, Kristin L. Main, Dustin C. Wade

Department of Chemistry and Biochemistry, University of North Carolina Wilmington, 601 S. College Road, Wilmington, NC 28403-5932, United States

Received 4 January 2006; received in revised form 20 February 2006; accepted 20 February 2006
Available online 28 February 2006

Abstract

The GIAO-HF method in Gaussian 03 was employed to calculate the isotropic NMR shielding values of a diatomic hydrogen probe above simple small-ring aromatic and antiaromatic hydrocarbons, including neutral and ionic examples. Subtraction of the isotropic shielding of diatomic hydrogen by itself allowed the prediction of through-space proton NMR shielding increment surfaces for these systems. Substantial shielding was observed above the center of aromatic rings, regardless of whether the ring was π-aromatic or σ-aromatic, and also regardless of the charge. In sharp contrast, deshielding was observed above the center of antiaromatic rings, regardless of whether the ring was π-aromatic or σ-aromatic, and also regardless of the charge. Shielding increment values at 2.5 Å above the ring centers were compared to NICS values at the same position. The shielding effects predicted by using diatomic hydrogen as a computational probe are diagnostic of whether a structure possesses aromaticity or antiaromaticity.

Keywords: NMR; Through-space shielding effects; GIAO; Aromatic; Antiaromatic; Hydrocarbon

1. Introduction

A number of approaches have been used since the concept of aromaticity was introduced by Kekulé 140 years ago [1] to describe whether a substance is aromatic or antiaromatic. In an introduction to a series of review articles on aspects of aromaticity, Schleyer [2] listed several methods. Aromaticity can be quantified by geometry observables (a measure of the similarity of ring CC bond lengths called the harmonic oscillator model of aromaticity, HOMA) [3–6], energy (aromatic stabilization energy, ASE) [7–11], magnetic properties (exhaltation of magnetic susceptibility, Λ [12–14], anisotropy of the magnetic susceptibility [15], nuclear magnetic shifts [16–18], and nucleus-independent chemical shifts, NICS, a measure of the diatropic (for aromatic compounds) or paratropic (for antiaromatic compounds) ring current) [19,20]. Aromatic ring current shieldings (ARCS) computed from NICS measurements perpendicular to the plane of aromatic rings have also been suggested as a measure of aromaticity [21]. Kleinpeter and Klod [22,23] used graphical maps of the anisotropy effect of aromatic rings, which they term isochemical shielding surfaces (ICSS), to confirm stereochemical assignments. The NICS concept has been expanded by Stanger [24] who introduced scanning NICS over a distance and partitioning them into in-plane and out-of-plane components. Cyrañsky et al. [25,26] showed that for a series of 75 five-membered ring π-electron systems and 30 ring-substituted compounds (including aromatic, nonaromatic and antiaromatic systems), loose correlations exist among the four most widely used measures of aromaticity: ASE, Λ, HOMA and NICS. To overcome limitations of each of these methods, Herges et al. [27] suggest using a graphical representation of the anisotropy of the induced current (ACID), which demonstrates electron delocalization, a universal attribute of aromaticity. Although no single measure of aromaticity is without limitations, the use of NICS has increased dramatically since it was developed [20].

We have previously reported the results of HF-GIAO calculations to calculate through-space NMR shielding effects, to map the resulting through-space NMR shielding increments, and to develop through-space NMR shielding equations for a number of common organic functional groups, including the benzene ring [28,29], the carbon–carbon double bond [30–33], the carbon–carbon triple bond, the carbon–nitrogen triple bond and the nitro group [34], the carbonyl group [35], and

* Corresponding author. Tel.: +1 910 962 3453; fax: +1 910 962 3013.
E-mail address: martinn@uncwil.edu (N.H. Martin).

1093-3263/$ – see front matter
doi:10.1016/j.jmgm.2006.02.006

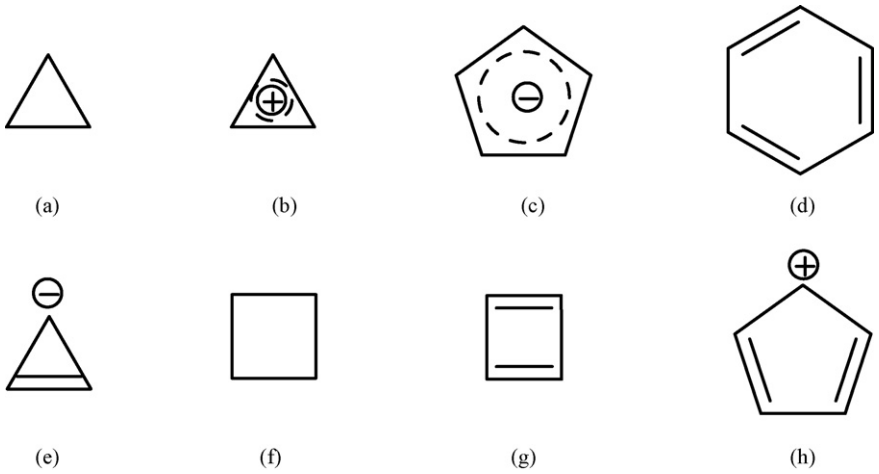

Fig. 1. Structures of the aromatic (top) and antiaromatic (bottom) small-ring hydrocarbons used in this study.

functional groups common to peptides [36]. The shielding predictions derived from calculations of small molecule models of those functional groups proved to be successful at accurately predicting through-space chemical shift effects in more complex molecules that contained those functional groups. We now report our computational study of the through-space NMR shielding of a diatomic hydrogen probe molecule by simple small-ring aromatic and antiaromatic hydrocarbons, including neutral and ionic examples.

2. Computational methods

Simple molecules and ions that are generally classified as either aromatic or antiaromatic were used as models. At the top of Fig. 1 are the aromatic structures cyclopropane (a), cyclopropenyl cation (b), cyclopentadienyl anion (c) and benzene (d). Below these are found the antiaromatic structures cyclopropenyl anion (e), cyclobutane (f), cyclobutadiene (g) and cyclopentadienyl cation (h). A model of each of these was built in Titan [37] on a Dell Dimension 3.31 GHz PC, then a geometry optimization calculation was performed at the Hartree–Fock level of theory using the 6-31G(d,p) basis set [38]. Most of these structures are planar which allowed the Cartesian coordinate molecule description to be located in the *XY* plane; for simplicity, cyclobutane was modeled with D_{4h} symmetry. A diatomic hydrogen (H_2) probe [39], previously geometry optimized at HF/6-31G(d,p), was placed along the *Z*-axis with the proximal hydrogen at a distance of 2.0 Å from the plane of each planar molecule. A series of single point NMR calculations[1] was performed in Gaussian 03 [40] on these supramolecules using the same method and basis set, moving the H_2 in 1.0 Å increments in both the *X*- and *Y*-directions in separate calculations. The process was repeated with the H_2 probe at proximate hydrogen distances of 2.5, 3.0 and 4.0 Å from the plane of the molecule being studied. These calculations covered a 3 Å × 3 Å grid in each quadrant (6 Å × 6 Å grid overall). The symmetry of these structures allowed only half (or one-fourth in some cases) of the grid to be calculated and the data to be replicated by a reflection across the *Y* (or *X* and *Y*) axis. Each of these structures was oriented with the carbon atoms in the *XY* plane with the center of the ring at the origin of Cartesian space.

The shielding increment ($\Delta\sigma$) at a given point in Cartesian space was determined by taking the difference between the calculated isotropic shielding value of one of the hydrogens in the H_2 probe alone (26.77 ppm) and that of the proximal hydrogen of the H_2 probe at that point relative to the modeled structures. Isotropic shift values greater than the calculated isolated H_2 isotropic shielding value (26.77 ppm) give positive (shielding) $\Delta\sigma$ values, and those with smaller values give negative (deshielding) $\Delta\sigma$ values. The shielding increments ($\Delta\sigma$) are therefore equal in magnitude but opposite in sign to differences in ^{1}H NMR chemical shifts ($\Delta\delta$). Three-dimensional NMR shielding increment surfaces ($\Delta\sigma$ versus *X* and *Y* at a fixed value of *Z*) were prepared using TableCurve 3D [41] to represent graphically the locations and magnitudes of shielding and deshielding regions over the molecules and ions in the study.

3. Results and discussion

In general, the ionic species showed the greatest shielding (or deshielding) effect, depending on the sign of the charge. Cations cause shielding effects, whereas anions cause deshielding effects on the proximate hydrogen atom of a nearby hydrogen molecule. This can be understood in terms of polarization of the H–H bond by the charge (Fig. 2). Also in general, aromatic rings cause shielding 2.5 Å over the center of the ring, whereas antiaromatic rings cause deshielding at that location. This simple measurement is diagnostic of aromaticity and antiaromaticity in the series of structures examined. This

[1] The difference between the shielding values obtained using single point calculations and constrained geometry-optimized calculations is negligible [39]. Also, previous calculations [31,34,35] have shown that basis set superposition error, as measured by the counterpoise method of Boys and Bernardi [42], has a negligible effect on shielding values. In the eight compounds in the current study, BSSE was no greater than 0.015 ppm.

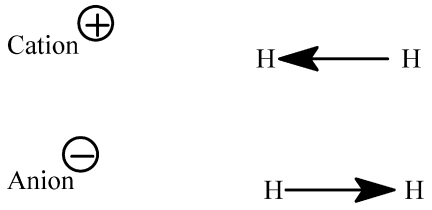

Fig. 2. Illustration of the induced polarization of the diatomic hydrogen probe molecule by a nearby charged species.

measure differs in sign and sometimes in magnitude from the commonly used NICS value. The major contributor to the difference in magnitude between these values is the electronic charge, to which NICS values are insensitive. The results of calculations of $\Delta\sigma$ and NICS values 2.5 Å from the isoelectronic Na^+, Ne, and F^- collected in Table 1 demonstrate this clearly.

Although calculations were performed with the hydrogen probe as close as 2.0 Å to the carbon skeleton of the ring, in cases where hydrogen atoms project above the plane of the ring carbons (e.g., cyclopropane and cyclobutane), severe distortion of the shielding increment surface was observed, presumably arising from van der Waals deshielding by the cycloalkane hydrogens. Distances closer than 2.5 Å encroach on the sum of the van der Waals radii of the probe hydrogen and the atoms (or π bonds) of the molecule or ions studied. Therefore, in the interest of uniformity of presentation, only the shielding increment surface data from proximal hydrogen distances of 2.5, 3.0, and 4.0 Å will be included in the discussion.

The 2.5 Å shielding increment surfaces of the aromatic structures (Fig. 1a–d) are shown in Fig. 3. The σ-aromatic cyclopropane (Fig. 3a and b) shows a mound of shielding at the center (maximum shielding increment at 2.5 Å is 0.97 ppm). This mound is surrounded by three smaller regions of deshielding (the minimum shielding increment at 2.5 Å is −0.40 ppm), each corresponding to the position of one of the hydrogens of cyclopropane projecting above the plane of the carbon skeleton. These smaller mounds are a consequence of van der Waals deshielding. At a hydrogen probe distance of 3.0 Å or greater (not shown), the localized structure of the shielding increment surface due to that deshielding effect is missing, and only the (nearly) circular mound of shielding due to the diatropic effect of the ring current arising from the σ-aromaticity of cyclopropane is apparent. The magnitude of maximum shielding diminishes as the distance of the probe from the carbon skeleton increases to 4.0 Å. The cyclopropenyl cation is π aromatic. At a distance of the hydrogen probe of 2.5 Å (Fig. 3c and d), the surface is a somewhat triangular mound of shielding (the maximum shielding at 2.5 Å is 2.28 ppm). At a distances of 3.0 and 4.0 Å (not shown), the mound of shielding diminishes in magnitude and becomes more circular. Because of the positive charge, the maximum shielding is still substantial (1.17 ppm) at 4.0 Å. The π-aromatic cyclopentadienyl anion has an interesting isotropic shielding increment surface (Fig. 3e and f). At a probe distance of 2.5 Å there is a pointed mound of shielding (the maximum shielding increment is 1.17 ppm) surrounded by regions of deshielding (the minimum shielding increment is −0.97 ppm). The shielding at the center is a consequence of the π-aromaticity of the ring. The surrounding deshielding regions result from the negative charge of the ion. As the distance of the hydrogen probe increases to 4.0 Å (not shown), the magnitude of shielding and deshielding diminish, but the general shape of the surface remains the same. We have previously reported the shielding surface of benzene [28] and of substituted aromatics [29] using methane as a computational probe. Using diatomic hydrogen as the probe, similar results are obtained, but the isotropic shielding increment values are slightly smaller [39]. The isotropic shielding increment surface for diatomic hydrogen over benzene at 2.5 Å is shown in Fig. 3g and h. A circular mound of shielding having a maximum shielding increment of 2.96 ppm is observed. As the probe distance increases, the magnitude of maximum shielding decreases, but the shape is retained (not shown).

Table 1
NICS and $\Delta\sigma$ values calculated at 2.5 Å from three isoelectronic species showing the effect of charge on $\Delta\sigma$ values but not on NICS values

Structure	NICS(2.5)	$\Delta\sigma_{2.5}$
Na^+	0.00	0.99
Ne	0.00	−1.09
F^-	0.00	−2.97

The isotropic shielding increment surfaces of the antiaromatic structures are collected in Fig. 4. The π-antiaromatic cyclopropenyl anion (Fig. 4a and b) has only deshielding regions in its isotropic shielding increment surfaces at any distance studied. With the proximal atom of the hydrogen probe at 2.5 Å above the carbon framework on the same side as the lone pair of electrons, a distinct region of greatest deshielding (the minimum shielding increment at 2.5 Å is −2.32 ppm) is observed in the vicinity of the anionic carbon, consistent with the localized nature of the charge in this ion. General deshielding throughout is a result of a combination of two effects: the negative charge and the presence of an alkene double bond [30–33]. As the distance of the hydrogen probe increases to 4.0 Å (not shown), the isotropic shielding increment surface becomes somewhat flatter and less featured. The σ-antiaromatic cyclobutane (Fig. 4c and d) shows the effects of van der Waals deshielding as well as the effects of the paratropic antiaromatic ring current. Four localized regions of deshielding (the minimum shielding increment at 2.5 Å is −1.03 ppm) correspond to the positions of the four cyclobutane hydrogens that project up from the plane of the carbon skeleton. As with cyclopropane, at distances of the hydrogen probe greater than 2.5 Å, the localized effects diminish so that at 4.0 Å a circular mound of deshielding is all that remains (not shown). This is the deshielding that results from the paratropic ring current of the σ-antiaromatic cyclobutane. The isotropic shielding increment surface of the π-antiaromatic cyclobutadiene is (Fig. 4e and f) shows an ellipsoidal trough of deshielding (the minimum shielding increment at 2.5 Å is −2.83 ppm) centered over the ring. This is likely the net result of two deshielding effects: the additive deshielding effect of the

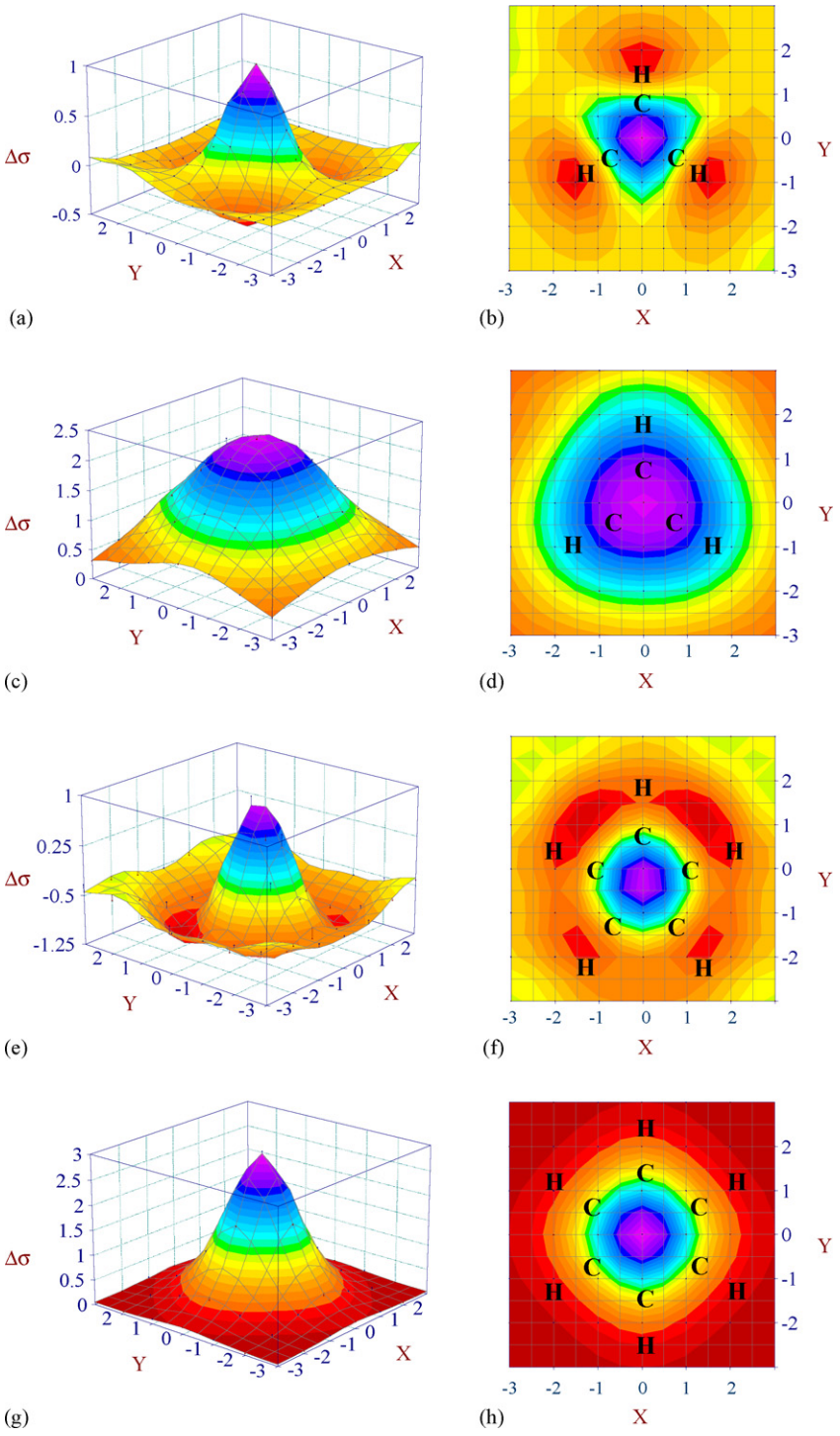

Fig. 3. Calculated isotropic NMR shielding increment surfaces (in ppm) of aromatic hydrocarbons: cyclopropane (a and b), cyclopropenyl carbocation (c and d), cyclopentadienyl anion (e and f) and benzene (g and h) using diatomic hydrogen as the probe molecule at 2.5 Å.

two π bonds and the paratropic (deshielding) effect of the antiaromatic ring current. The deshielding trough diminishes in magnitude as the probe distance increases (not shown), but the shape remains ellipsoidal. In the shielding increment surface of the π-antiaromatic cyclopentadienyl cation (Fig. 4g and h) the shielding effect of the localized positive charge is evident as a slight mound centered above the hydrogen attached to the positive (top) carbon. This feature is dwarfed by the deep trough of deshielding (the minimum isotropic shielding increment at 2.5 Å is −3.87 ppm) near the ring center. The shape of the shielding increment surface is retained but with diminishing amplitude as the probe distance increases to 4.0 Å (not shown).

Table 2 summarizes the calculated maximum shielding increment values of the H_2 probe at each of the distances from the simple models of aromatic and antiaromatic hydrocarbons

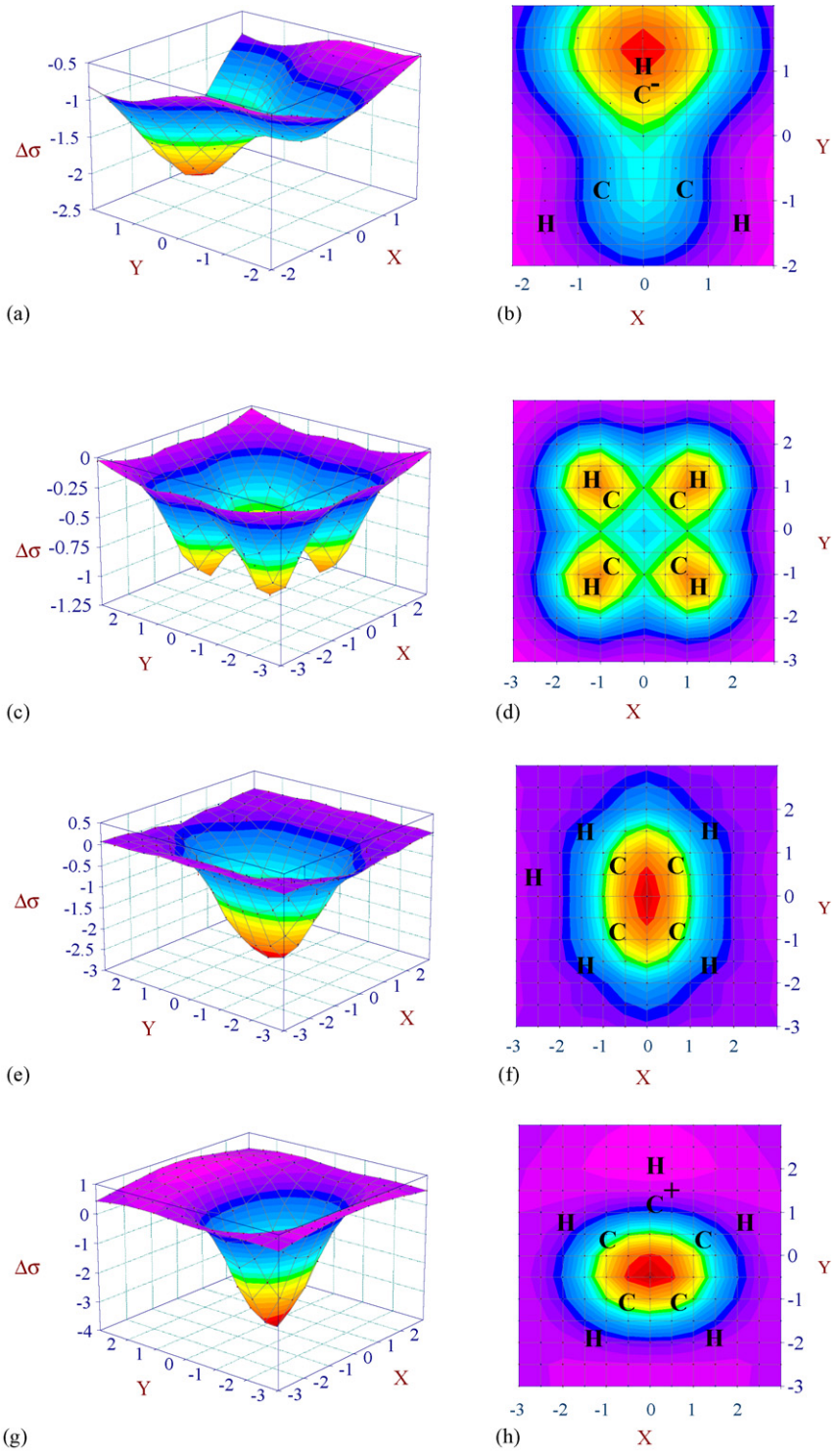

Fig. 4. Calculated isotropic NMR shielding increment surfaces (in ppm) of antiaromatic hydrocarbons: cyclopropenyl anion (a and b), cyclobutane (c and d), cyclobutadiene (e and f) and cyclopentadienyl cation (g and h) using diatomic hydrogen as the probe molecule at 2.5 Å.

included in the study. Also found in Table 2 are the nucleus independent chemical shielding values (NICS) and shielding increment values ($\Delta\sigma$), both calculated at 2.5 Å above the center of each ring. Aside from the sign difference which results from the conventions used, the two measurements agree for the most part. Differences between $\Delta\sigma_{2.5}$ and NICS(2.5) arise in part because NICS values are insensitive to charge (vide supra), whereas $\Delta\sigma_{2.5}$ values are not. One case where the sign of the NICS is inconsistent with the prediction of antiaromaticity is the cyclopropenyl anion. The NICS(2.5) value is −0.54; the $\Delta\sigma_{2.5}$ value is −1.54, same sign, but greater magnitude, consistent with the added deshielding effect of the negative

Table 2
Maximum isotropic shielding increment values (ppm) of the H_2 probe at 2.5, 3.0, and 4.0 Å from simple models of aromatic and antiaromatic hydrocarbons, isotropic shielding increment values ($\Delta\sigma$) and NICS both calculated at 2.5 Å above the center of each ring

Model structure	Distance from H_2 probe (Å)				
	2.5	3.0	4.0	$\Delta\sigma_{2.5}$	NICS(2.5)
Cyclopropane	0.97	0.58	0.23	0.97	−0.97
Cyclopropenium cation	2.28	1.96	1.17	2.28	−1.63
Cyclobutane	−0.03	−0.03	−0.03	−0.52	0.49
Cyclopropenyl anion	−0.53	−0.41	−0.32	−1.56	−0.58
Cyclobutadiene	0.11	0.03	−0.01	−2.83	2.08
Cyclopentadienyl anion	1.17	0.24	−0.12	1.17	−2.62
Cyclopentadienyl cation	0.97	0.62	0.37	−3.87	4.27
Benzene	2.96	1.83	0.84	2.96	−3.30

charge. Another major difference between NICS and $\Delta\sigma$ values is that the latter (but not NICS) measure a shielding increment on a covalently bonded nucleus, and it has been demonstrated using IGLO calculations that from 27 to 67% of the shielding experienced by that nucleus arises from orbitals associated with that nucleus [43]. The $\Delta\sigma_{2.5}$ values provide a simple diagnostic test of aromaticity (or antiaromaticity) in the structures studied. Positive $\Delta\sigma_{2.5}$ values are associated with aromatic ring structures; negative values are associated with antiaromatic structures. This trend holds even in the cases of ionic species where the effect of the charge opposes the ring current effect. Only in cyclobutane and cyclopropenyl anion are the $\Delta\sigma_{2.5}$ values different from the maximum or minimum isotropic shielding increment value at that distance. In cyclobutane, greater deshielding arises from van der Waals deshielding by the four hydrogen atoms than from the paratropic antiaromatic ring current effect. The cyclopropenyl anion has the maximum deshielding near the anionic carbon rather than over the center of the ring, where the smaller paratropic antiaromatic ring current effect appears.

Table 3 summarizes the calculated minimum shielding increment values of the H_2 probe at each of the distances from the simple models of aromatic and antiaromatic hydrocarbons included in the study (note that a negative $\Delta\sigma$ represents deshielding).

Table 3
Minimum isotropic shielding increment values (ppm) of the H_2 probe at 2.5, 3.0, and 4.0 Å from simple models of aromatic and antiaromatic hydrocarbons (negative values indicate deshielding)

Model structure	Distance from H_2 probe (Å)		
	2.5	3.0	4.0
Cyclopropane	−0.40	−0.02	0.01
Cyclopropenium cation	0.30	0.33	0.34
Cyclobutane	−1.03	−0.38	−0.20
Cyclopropenyl anion	−2.32	−1.33	−0.66
Cyclobutadiene	−2.83	−1.43	−0.53
Cyclopentadienyl anion	−0.97	−0.50	−0.29
Cyclopentadienyl cation	−3.87	−1.51	−0.28
Benzene	−0.01	0.04	0.09

4. Conclusions

Diatomic hydrogen (H_2) was used as a computational probe of the through-space NMR shielding of small ring aromatic and antiaromatic hydrocarbons. The isotropic shielding increment ($\Delta\sigma$) of the proximal hydrogen plotted against the X and Y Cartesian coordinates give isotropic shielding increment surfaces. Aromatic rings show a distinct mound of shielding (positive $\Delta\sigma$) centered over the ring, whereas antiaromatic rings show a mound of deshielding (negative $\Delta\sigma$) similarly placed. These mounds may be superimposed on general shielding or deshielding surfaces that arise from local effects, such as van der Waals deshielding due to nearby hydrogens that project above the carbon skeleton (as in the case of cyclopropane and cyclobutane) or the effect of ionic charge. Positively charged ions cause general shielding, whereas negatively charged ions cause deshielding of the proximal hydrogen of the diatomic hydrogen probe molecule. The isotropic shielding increment ($\Delta\sigma$) of the proximal hydrogen measured at 2.5 Å above the ring center of each structure ($\Delta\sigma_{2.5}$) is diagnostic for whether a ring structure is aromatic or antiaromatic. Although $\Delta\sigma_{2.5}$ values are sensitive to charge, the major factor in the series studied is aromaticity or antiaromaticity. Aromatic rings have positive values of $\Delta\sigma_{2.5}$ whereas antiaromatic rings have negative values of $\Delta\sigma_{2.5}$.

References

[1] A. Kekulé, Sur la constitution des substances aromatiques, Bull. Soc. Chim. Fr. (Paris) 3 (2) (1865) 98–110.
[2] P.v.R. Schleyer, Introduction: aromaticity, Chem. Rev. 101 (5) (2001) 1115–1118.
[3] T.M. Krygowski, Crystallographic studies of inter- and intramolecular interactions reflected in aromatic character of p-electron systems, J. Chem. Inf. Comput. Sci. 33 (1) (1993) 70–78.
[4] T.M. Krygowski, M.K. Cyrañsky, Separation of the energetic and geometric contributions to the aromaticity of π-electron carbocyclics, Tetrahedron 52 (5) (1996) 1713–1722.
[5] T.M. Krygowski, M.K. Cyrañsky, Aromatic character of carbocyclic π-electron systems deduced from molecular geometry, in: M. Hargittai, I. Hargittai (Eds.), Advances in Molecular Structure Research, vol. 3, JAI Press, London, 1997, pp. 227–268.
[6] T.M. Krygowski, M.K. Cyranski, Structural aspects of aromaticity, Chem. Rev. 101 (5) (2001) 1385–1419.
[7] W.J. Hehre, R.T. McIver, J.A. Pople, P.v.R. Schleyer, Alkyl substituent effects on the stability of protonated benzene, J. Am. Chem. Soc. 96 (1974) 7162–7163.
[8] P. George, M. Trachtman, A.M. Brett, C.W. Bock, Comparison of various isodesmic and homodesmotic reaction heats with values derived from published ab initio molecular orbital calculations, J. Chem. Soc., Perkin Trans. 2 (1977) 1036–1047.
[9] C.H. Suresh, N. Koga, Accurate calculation of aromaticity of benzene and antiaromaticity of cyclobutadiene: new homodesmotic reactions, J. Org. Chem. 67 (2002) 1965–1968.
[10] L.J. Schaad, B.A. Hess Jr., Dewar resonance energy, Chem. Rev. 101 (5) (2001) 1465–1476.
[11] J.F. Liebman, S.W. Slayden, The energetics of aromatic hydrocarbons: an experimental thermochemical perspective, Chem. Rev. 101 (5) (2001) 1541–1566.
[12] H.J. Dauben, J.D. Wilson, J.L. Laity, Diamagnetic susceptibility exaltation as a criterion of aromaticity, J. Am. Chem. Soc. 91 (8) (1969) 1991–1998.
[13] J. Hoarau, Magnetic properties of conjugated molecules, J. Ann. Chim. 13 (1) (1956) 544–587.

[14] A. Pacault, Magnetochemical studies A, Ann. Chim. 12 (1) (1946) 527–587.
[15] W.H. Flygare, Magnetic interactions in molecules and an analysis of molecular electronic charge distribution from magnetic parameters, Chem. Rev. 74 (1974) 653–687.
[16] C.W. Haigh, R.B. Mallion, Ring current theories in nuclear magnetic resonance, in: J.W. Emsley, J. Feeny, L.H. Sutcliffe (Eds.), Progress in Nuclear Magnetic Resonance Spectroscopy, vol. 13, Pergamon Press, Oxford, U.K, 1979/1980.
[17] J.A.N.F. Gomes, R.B. Mallion, The concept of ring currents, in: D.H. Rouvray (Ed.), Concepts in Chemistry: A Contemporary Challenge, Research Studies Press, Taunton, Somerset, UK, 1997, pp. 205–253.
[18] P. Lazzeretti, Ring currents, in: J.W. Emsley, J. Feeny, L.H. Sutcliffe (Eds.), Progress in Nuclear Magnetic Resonance Spectroscopy, vol. 36, Elsevier, Amsterdam, The Netherlands, 2000, pp. 1–88.
[19] P.v.R. Schleyer, C. Maerker, A. Dransfield, H. Jiao, N.J.R. van Eikema Hommes, Nucleus-independent chemical shifts: a simple and efficient aromaticity probe, J. Am. Chem. Soc. 118 (1996) 6317–6318.
[20] Z. Chen, C.S. Wannere, C. Corminboeuf, R. Puchta, P.v.R. Schleyer, Nucleus-independent chemical shifts (NICS) as an aromaticity criterion, Chem. Rev. 105 (10) (2001) 3842–3888.
[21] J. Jusélius, D. Sundholm, Ab initio determination of the induced ring current in aromatic molecules, Phys. Chem. Chem. Phys. 1 (1999) 3429–3435.
[22] S. Klod, E. Kleinpeter, Ab initio calculation of the anisotropy effect of multiple bonds and the ring current effect of arenes-application in conformational and configurational analysis, J. Chem. Soc., Perkin Trans. 2 (2001) 1893–1898.
[23] E. Kleinpeter, S. Klod, Ab initio calculation of the anisotropic/ring current effects of amino acid residues to locate the position of substrates in the binding site of enzymes, J. Mol. Struct. 704 (2004) 79–82.
[24] A. Stanger, Nucleus-independent chemical shifts (NICS): distance dependence and revised criteria for aromaticity and antiaromaticity, J. Org. Chem. 71 (3) (2006) 883–893.
[25] M.K. Cyrañsky, T.M. Krygowski, A.R. Katritsky, P.v.R. Schleyer, To what extent can aromaticity be defined uniquely? J. Org. Chem. 67 (4) (2002) 1333–1338.
[26] M.K. Cyrañski, Energetic aspects of cyclic pi-electron delocalization: evaluation of the methods of estimating aromatic stabilization energies, Chem. Rev. 105 (10) (2005) 3773–3811, and references cited therein.
[27] D. Geuenich, K. Hess, F. Köhler, R. Herges, Anisotropy of the induced current density (ACID), a general method to quantify and visualize electronic delocalization, Chem. Rev. 105 (10) (2005) 3758–3772, and references cited therein.
[28] N.H. Martin, N.W. Allen III, K.D. Moore, L. Vo, A proton NMR shielding model for the face of a benzene ring, J. Mol. Struct. (Theochem.) 454 (1998) 161–166.
[29] N.H. Martin, N.W. Allen III, J.C. Moore, An algorithm for predicting NMR shielding of protons over substituted benzene rings, J. Mol. Graphics Mod. 18 (3) (2000) 242–246.
[30] N.H. Martin, N.W. Allen III, E.K. Minga, S.T. Ingrassia, J.D. Brown, An empirical proton NMR shielding equation for alkenes based on ab initio calculations, Struct. Chem. 9 (6) (1998) 403–410.
[31] N.H. Martin, N.W. Allen III, E.K. Minga, S.T. Ingrassia, J.D. Brown, A new proton shielding model for alkenes, in: Proceedings of the ACS symposium on Modeling NMR Chemical Shifts: Gaining Insights into Structure and Environment, ACS Press, 1999, pp. 207–219.
[32] N.H. Martin, N.W. Allen III, E.K. Minga, S.T. Ingrassia, J.D. Brown, An improved model for predicting proton NMR shielding by alkenes based on ab initio GIAO calculations, Struct. Chem. 10 (5) (1999) 375–380.
[33] N.H. Martin, N.W. Allen III, S.T. Ingrassia, J.D. Brown, E.K. Minga, An algorithm for predicting proton deshielding over a carbon–carbon double bond, J. Mol. Graphics Modell. 18 (1) (2000) 1–6.
[34] N.H. Martin, K.H. Nance, Modeling through-space magnetic shielding over the ethynyl, cyano, and nitro groups, J. Mol. Graphics Modell. 21 (2002) 51–56.
[35] N.H. Martin, N.W. Allen III, J.D. Brown, D.M. Kmiec Jr., L. Vo, An NMR shielding model for protons above the plane of a carbonyl group, J. Mol. Graphics Modell. 22 (2003) 127–131.
[36] N.H. Martin, D.M. Loveless, K.L. Main, A.K. Pyles, Computation of through-space shielding effects by functional groups common to peptides, J. Mol. Graphics Modell., in press.
[37] Titan, version 1.0.1, Wavefunction, Inc./Schrödinger, Inc., 1999.
[38] W.J. Hehre, L. Radom, P.v.R. Schleyer, J.A. Pople, Ab Initio Molecular Orbital Theory, Wiley, New York, 1986.
[39] N.H. Martin, D.M. Loveless, D.C. Wade, A comparison of calculated NMR shielding probes, J. Mol. Graphics Modell. 23 (2004) 285–290.
[40] M.J. Frisch, G.W. Trucks, H.B. Schlegel, G.E. Scuseria, M.A. Robb, J.R. Cheeseman, J.A. Montgomery Jr., T. Vreven, K.N. Kudin, J.C. Burant, J.M. Millam, S.S. Iyengar, J. Tomasi, V. Barone, B. Mennucci, M. Cossi, G. Scalmani, N. Rega, G.A. Petersson, H. Nakatsuji, M. Hada, M. Ehara, K. Toyota, R. Fukuda, J. Hasegawa, M. Ishida, T. Nakajima, Y. Honda, O. Kitao, H. Nakai, M. Klene, X. Li, J.E. Knox, H.P. Hratchian, J.B. Cross, C. Adamo, J. Jaramillo, R. Gomperts, R.E. Stratmann, O. Yazyev, A.J. Austin, R. Cammi, C. Pomelli, J.W. Ochterski, P.Y. Ayala, K. Morokuma, G.A. Voth, P. Salvador, J.J. Dannenberg, V.G. Zakrzewski, S. Dapprich, A.D. Daniels, M.C. Strain, O. Farkas, D.K. Malick, A.D. Rabuck, K. Raghavachari, J.B. Foresman, J.V. Ortiz, Q. Cui, A.G. Baboul, S. Clifford, J. Cioslowski, B.B. Stefanov, G. Liu, A. Liashenko, P. Piskorz, I. Komaromi, R.L. Martin, D.J. Fox, T. Keith, M.A. Al-Laham, C.Y. Peng, A. Nanayakkara, M. Challacombe, P.M.W. Gill, B. Johnson, W. Chen, M.W. Wong, C. Gonzalez, J.A. Pople, Gaussian 03, Revision B.01, Gaussian, Inc., Pittsburgh, PA, 2003
[41] TableCurve3D, version 3.00A, AISN Software, San Rafael, CA, 1997.
[42] S.F. Boys, F. Bernardi, The calculations of small molecular interaction by the difference of separate total energies. Some procedures with reduced error, Mol. Phys. 19 (1970) 553–566.
[43] N.H. Martin, J.D. Brown, K.H. Nance, H.F. Schaefer III, P.v.R. Schleyer, Z.-X. Wang, H.L. Woodcock, Analysis of the origin of through-space NMR (de)shielding by selected organic functional groups, Org. Lett. 3 (24) (2001) 3823–3826, and references cited therein.